Southern High Plains Texas Agriculture

Cover Cropping Mapping in the Southern High Plains of Texas

Fall 2025 | Colorado – Fort Collins
November 21st, 2025

Authors: Jaya Hafner (Analytical Mechanics Associates), Dorothy Janick (Analytical Mechanics Associates), Oliver Matus-Bond (Analytical Mechanics Associates), Shawronna Sengupta (Analytical Mechanics Associates)

Abstract: The Southern High Plains of Texas is a semi-arid agricultural region that is vulnerable to soil erosion and water scarcity. Winter cover cropping, the practice of sowing crops during the winter season specifically for ecological benefits rather than for harvest, is a potential strategy for reducing erosion. However, trends in cover crop adoption and their effects on water dynamics in the region are insufficiently understood. In partnership with the Sandhills Area Research Association, Bamert Seed Company, and Texas A&M AgriLife, the NASA DEVELOP team used field data from farmers and Harmonized Landsat and Sentinel-2 (HLS) imagery to test the feasibility of mapping winter cover cropping in the region, characterize spatial patterns in winter cover crop adoption, and explore evapotranspiration and soil moisture trends on winter cover cropped fields using a research site as a case study. The team developed a random forest model to detect winter cover-cropped fields and compared outputs to a cover crop classification algorithm that collaborators at the United States Department of Agriculture and United States Geological Survey initially developed for Maryland. The model results indicated that cover crop mapping in the region was improved by incorporating diverse vegetation and soil indices, termination detection, and field data from farmers. Preliminary results from satellite-derived evapotranspiration and soil moisture data showed that cover crops impact water availability, but further validation is needed. These results supported the partners in evaluating cover crop adoption, assessing cover crop impacts on water supply, and informing future research in the region.

Key Terms: remote sensing, winter cover cropping, random forest, evapotranspiration, soil moisture, Harmonized Landsat and Sentinel-2

Advisors: Dr. Anthony Vorster (Colorado State University, Natural Resource Ecology Laboratory), Dr. Paul Evangelista (Colorado State University, Natural Resource Ecology Laboratory), Christopher Tsz Hin Choi (Colorado State University, Natural Resource Ecology Laboratory)

Lead: Truman Anarella (Colorado – Fort Collins) and Kaitlyn Lemon (DEVELOP NPO)

1. Introduction

1.1 Background

The Southern High Plains of Texas is a semi-arid region characterized by low annual rainfall, clay to sandy loam soils, and flat plains (Cronin & Myers, 1964; Texas Almanac, 2021). As a result of the region's topography, long growing seasons, fertile soil, and proximity to the Ogallala Aquifer, agriculture is the primary industry, dominated by cotton production (Soil Health Institute, 2023). In the early twentieth century, farmers converted large areas of native rangeland to cropland, replacing deep-rooted perennial vegetation, which previously anchored the soil, with seasonal cropping systems. This land use exposes soil to erosion, especially during fallow periods, when fields are bare and unprotected. At the same time, the region's dependence on the Ogallala Aquifer for irrigating water-intensive cotton has contributed to declining groundwater levels, as extraction has exceeded natural recharge (Allen, 2004; Texas Parks and Wildlife Department, n.d.).

One solution to addressing soil erosion is cover cropping over the winter season. Cover cropping is the practice of sowing crops specifically for ecological benefits rather than for harvest. By covering the soil during the off-season and stabilizing it with their root systems, cover crops reduce soil erosion. Cover cropping can also improve soil health, enhance nutrient cycling and carbon storage, and reduce runoff and nitrogen loss (Yousefi et al., 2024). The performance of cover crops varies with crop type, climate conditions, and management practices such as tillage and termination method. Some studies reported that cover cropping improves subsequent crop water use efficiency by up to 5% through reduced evapotranspiration, though this effect may differ in dryland areas where there are higher evapotranspiration rates (Yousefi et al., 2024). In Lubbock County, Baxter et al. (2021) found that no-till cover crops did not reduce soil moisture compared to fallow areas, based on field measurements. However, regional trends in cover crop adoption and their effects on water supply are insufficiently understood.

1.2 Remote Sensing

Remote sensing approaches provide an opportunity to extend analyses of cover cropping across multiple counties in Texas. Previous studies, including Ahmed et al. (2023) and Hively et al. (2015), demonstrated that spectral indices like the Normalized Difference Vegetation Index (NDVI) are effective for detecting winter cover crop vegetation, crop residue, and tillage patterns. Additional studies demonstrated that it is feasible to use remotely sensed surface temperature and reflectance data to calculate the surface energy balance and estimate evapotranspiration of agricultural crops (Allen et al., 2007; Laipelt et al., 2021). Building on these methods, this project aimed to test the feasibility of mapping winter cover cropping in the Southern High Plains of Texas, characterize spatial patterns in winter cover crop adoption, and explore evapotranspiration and soil moisture trends on winter cover cropped fields using a research site as a case study.

1.3 Partners

To conduct this study, the team partnered with the Sandhills Area Research Association (SARA), Bamert Seed Company, and Texas A&M AgriLife Research. SARA, a non-profit organization that supports the region's agricultural community and advances sustainability through educational programs and partnerships, wanted to explore how remote sensing techniques can provide insights on cover cropping in the region. Bamert Seed Company is a private company that breeds and supplies native seeds, including varieties locally grown as cover crops. The company was interested in better understanding how cover cropping influences water supply in the region, which could guide their approach to cover crop selection and use. Texas A&M AgriLife Research, a state agricultural research agency within the Texas A&M University System, sought to gather more data on the benefits and tradeoffs of cover cropping in the region so that they can share evidence-based insights with farmers making management decisions. The team also collaborated with researchers at the United States Department of Agriculture (USDA) Agricultural Research Service (ARS) and the United States Geological Survey (USGS) who have been developing a remote sensing cover crop classification algorithm for Maryland (Maryland Model). By applying the Maryland Model algorithm to the Southern High Plains of Texas and comparing its outputs to those from a random forest model that the team

developed specifically for the region, the team aimed to provide resources that directly support partners in evaluating cover crop adoption and its impacts in the region.

1.4 Study Area

The study area covered eight counties in the Southern High Plains of Texas: Bailey, Lamb, Hale, Hockley, Lubbock, Terry, Lynn, and Dawson (Figure 1). The High Plains of Texas receive approximately 12 to 21 inches of rainfall a year, with periodic drought conditions and extreme windstorms (Allen, 2004; Texas Parks and Wildlife Department, n.d.). The study period for the cover crop mapping spanned from 2024 to 2025 to align with availability of results from the Maryland Model. The study period for the evapotranspiration and soil moisture case study spanned from 2016 to 2024 to align with availability of Landsat and OpenET data.

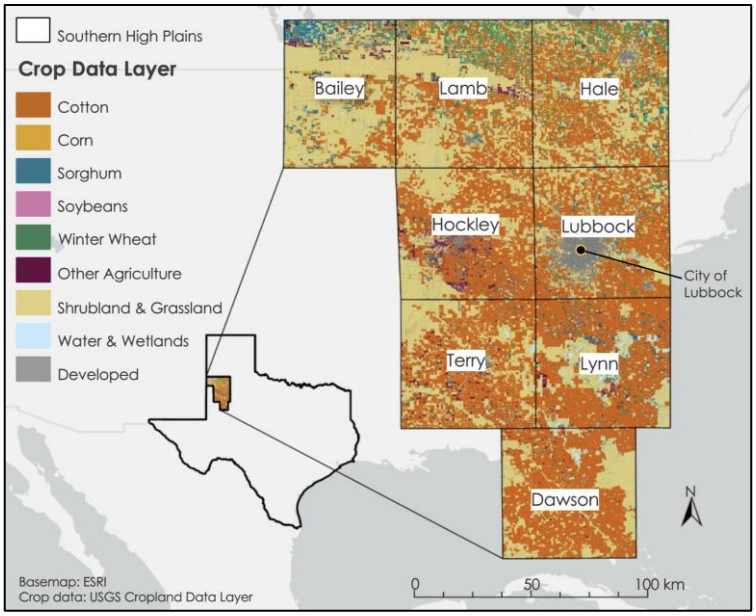

Figure 1. The study area covered eight counties in the Southern High Plains of Texas: Bailey, Lamb, Hale, Hockley, Lubbock, Terry, Lynn, and Dawson.

2. Methodology

2.1 Data Acquisition

To define the study area, the team acquired Texas county polygons from the Texas Department of Transportation's open data portal (Texas Department of Transportation, 2025). The team acquired crop information for the eight counties of interest from the 2024 Cropland Data Layer (CDL) using the USDA's CropScape web service (USDA National Agricultural Statistics Service, 2024). The CDL provided annual crop-specific land cover information at 30-meter resolution based on the year of harvest. The dataset was created from a combination of satellite imagery and ground reference data. The 2024 CDL included over 130 categories for crop types, as well as a "cultivated layer" that classified pixels based on whether they were cultivated or not from 2020 to 2024.

For assessing winter cover crop adoption in the study area, the team acquired a raster file containing outputs from the Maryland Model, which the USDA-ARS and USGS collaborators had applied to the Texas study area for the 2024–2025 winter season. The model used satellite imagery from the Harmonized Landsat and Sentinel-2 (HLS) product to detect seasonal patterns at 30-meter resolution. It assigned each pixel a value from 1 to 10 to represent the likelihood that the pixel had a winter cover crop, with 10 corresponding to the highest likelihood, a value of 255 if no winter cover crop was detected, or a value of 253 if there was no data available for that pixel.

To both explore the Maryland Model outputs and to build a new random forest classification model tailored to the study area, the team used Google Earth Engine to acquire surface reflectance data from Harmonized Landsat Sentinel-2 Operational Land Imager Surface Reflectance and TOA Brightness Daily Global 30m v2.0 (Masek et al., 2021). The HLS product combines data from sensors aboard NASA and European Space Agency (ESA) satellites, including Landsat 8's Operational Land Imager (OLI), Landsat 9's OLI-2, and Sentinel-2's Multi-Spectral Instrument (MSI; Table 1). Combined, HLS provides observations every two to three days at 30-meter resolution. Using Google Earth Engine, the team retrieved images of the study area between 2024 and 2025.

Partners at SARA and Texas A&M AgriLife provided essential field data on cover cropping practices in the study area. They shared survey responses from farmers with information on locations and farm management history for eleven fields, five of which had data from the 2024–2025 season. Texas A&M AgriLife provided detailed management information from 2014 through 2025 for four research fields within the Agricultural Complex for Advanced Research and Extension Systems (AG-CARES). The AG-CARES site included adjacent winter cover cropped and non-covered fields with similar soil types and environmental conditions. The field composition and comprehensive management data made it an ideal site for a case study exploring the relationship between winter cover cropping, evapotranspiration, and soil moisture.

The team acquired evapotranspiration data through Google Earth Engine's data catalog from 2016 to 2024 from OpenET Ensemble Monthly Evapotranspiration v2.0 (Melton et al., 2021), which used outputs from six evapotranspiration models (Table A1). Each model produced an estimate of the monthly total water, in millimeters, transferred from the land to the atmosphere via evapotranspiration at a 30-meter resolution. OpenET's ensemble model averaged total millimeters per month across the six models and removed outliers using the median absolute deviation method described in Hampel (1974). Earth observations for the six evapotranspiration models primarily came from Landsat thermal and optical imagery. To gather data needed for soil moisture analysis, the team used Google Earth Engine to acquire Landsat 8 Operational Land Imager and Thermal Infrared Sensor (OLI/TIRS) and Landsat 9 OLI-2/TIRS-2 for both surface reflectance and land surface temperature (Table 1).

Table 1
Earth observations

Platform & Sensor	**Data Type & Resolution**
Landsat 8 OLI & TIRS	Surface reflectance and land surface temperature; 30-meter resolution, 16-day revisit time
Landsat 9 OLI-2 & TIRS-2	Surface reflectance and land surface temperature; 30-meter resolution, 16-day revisit time
Sentinel-2 MSI	Surface reflectance; 10-meter resolution, 2–3-day revisit time

2.2 Data Processing

2.2.1. Maryland Model

Preparing the Maryland Model outputs for analysis involved using ArcGIS Pro (3.5.0) to clip the raster file to the CDL's "cultivated layer," thereby filtering the model results to cultivated land only. To explore the model's predictions for cropland planted with different cash crops, the team created crop masks for the three most prevalent crops in the study area: corn, cotton, and sorghum. These masks were created by reclassifying the crop values in the CDL so that the crop type of interest was assigned a value of "1" and all other crop types were assigned as "no data." In Maryland, where the model was initially refined, a likelihood score of 3 or above usually indicated the presence of winter cover crops. To assess how the Maryland Model's likelihood threshold performed in the study area, the team used ArcGIS Pro to reclassify the clipped Maryland Model raster and create a binary mask. The binary mask assigned all pixels with a likelihood score of 3 and above a value of "1," and all other pixels were assigned a "no data" value. Additionally, to enable comparison between the model outputs and the nine fields with farmer-provided management data, the team used ArcGIS Pro to

manually create polygons for the five production fields and four research fields with 2024–2025 data, with a 30-meter inward buffer to avoid contamination from edge pixels.

2.2.2. Random Forest Model

Preparing the acquired datasets for the random forest model involved three main steps: processing the HLS imagery, generating training data, and preparing predictor variables. To process the acquired HLS imagery, the team developed a script in Google Earth Engine to mask out clouds and cloud shadows by scaling reflectance values to top-of-atmosphere reflectance by multiplying them by 0.0001 and removing blue band and shortwave infrared band pixels that were too bright and had a reflectance value of less than 0.25. With the cloud mask applied, the team's script used the cloud-free pixels to create a monthly composite using the median value of each spectral band for each pixel. The team then used this processed imagery as part of the training data generation process.

Random forest classification models are ensemble learning models that learn to classify new data based on a set of training data. Generally, more training points lead to greater accuracy. The farmer-provided data on five fields in the study area with 2024–2025 data were highly valuable for validating the model's results, though the sample size was limited for training a model, so the team developed a process to generate training points. The team used ArcGIS Pro to generate 304 random points within the "cultivated layer" of the CDL in the study area, divided equally across the eight counties. The randomized points were then imported into Google Earth Engine, where the team's script generated two median composites of HLS true-color imagery for the months of February and May, 2025. Using this imagery, the team visually inspected each randomized data point and recorded whether the field that the point was located within appeared green or brown in February and in May, as well as which crop the CDL reported was harvested from that pixel in 2024. If a pixel appeared green in February but brown in May, it was classified as having a winter cover crop. These months were selected because February was when cover crop vegetation typically peaked in the study area, as analyses of the ground-truth data showed, and May was after winter cover crops were usually terminated but before summer crops emerged (Figure 2). Some crops in the study area, like winter wheat, are commonly planted in the fall, grown over the winter and spring, then harvested in the summer. While such crops do provide winter cover, for the purpose of this project, winter crops were only considered cover crops if they were terminated in the spring, rather than grown for later harvest. Consequently, fields that were green in both February and May were not classified as winter cover crops.

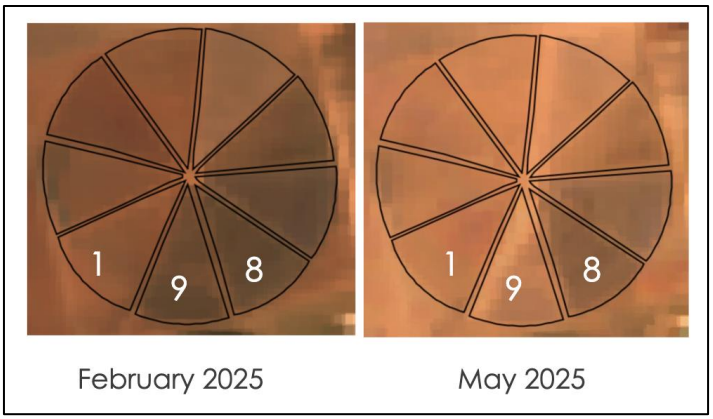

Figure 2. True-color HLS images of the AG-CARES research field in February and May 2025. Field 1 did not use cover cropping, Field 9 had cereal rye cover crop planted in winter and terminated in spring, and Field 8 was planted with winter wheat for summer harvest.

The majority of the 304 randomized points were classified as not having winter cover crops. To gain a better balance in the training data, the team opportunistically selected 145 additional points, covering pixels that showed evidence of winter cover crops as well as pixels that showed evidence of winter cover that was not

terminated in the spring. Because termination is an essential feature of winter cover cropping, the team sought to generate enough training data for the model to learn to differentiate between winter cash crops grown for summer harvest and winter cover crops that were terminated in the spring. In total, the team generated 449 points, which included 156 points with winter cover crops, 35 points with winter cash crops that were still green in May, and 258 points that had no winter cover. These data points were then imported into Google Earth Engine to train the random forest model.

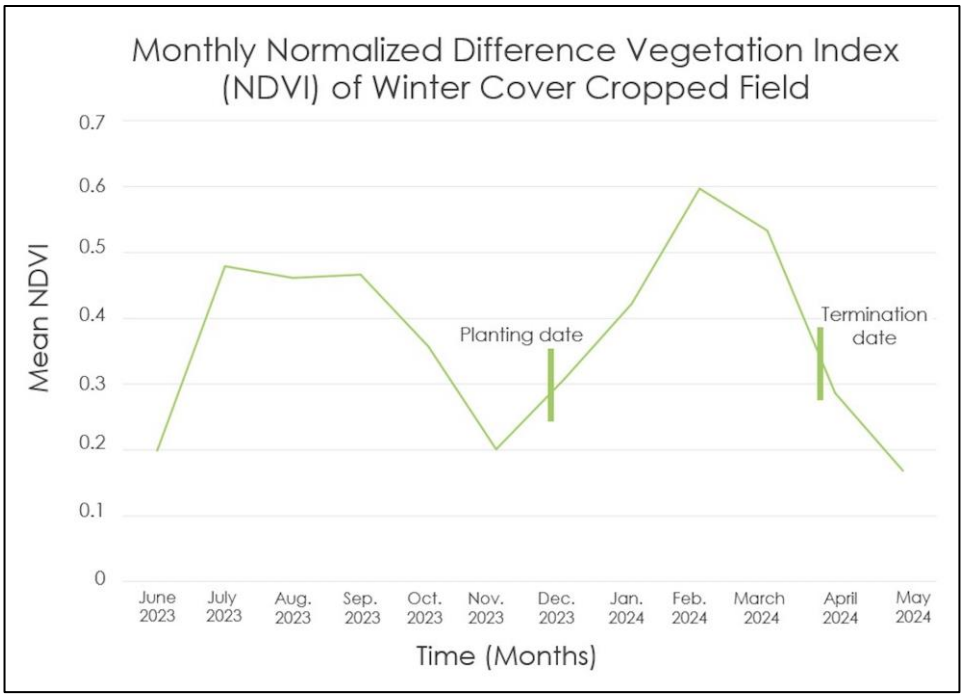

Figure 3. Monthly NDVI of a winter cover cropped field with cover crop planting and termination dates provided by the farmer.

Random forest classification models require a defined set of predictors, which are features used to predict how to classify each new data point. To build the random forest model, the team developed a Google Earth Engine script that selected thirteen predictors based on five indices (Table A2). These predictors were selected due to their capacities to detect seasonal patterns associated with winter cover cropping, like changes in NDVI (Figure 3). NDVI calculates the difference between spectral values in the near-infrared and red bands, and it can serve as a proxy for vegetative health (Equation 1; Rouse et al., 1973). The random forest used seven predictors based on NDVI, including median NDVI, minimum and maximum NDVI in the previous summer, minimum and maximum NDVI in the winter, the difference in median NDVI between February and May, and the difference in peak NDVI in February–March and low NDVI in April–May. The random forest model used two predictors based on the Normalized Burn Ratio (NBR) and the Bare Soil Index (BSI). NBR uses reflectance in the near-infrared and short-wave infrared bands to assess burn severity and burned areas, which can serve as a proxy for bare soil to enable cover crop termination detection (Equation 2; Key & Benson, 2006). BSI identifies areas with bare soil by calculating relationships between the shortwave infrared, near-infrared, red, and blue bands (Equation 3; Rikimaru et al., 2002). The predictors for NBR and BSI calculated the difference in index values between February and May as well as the difference between the peak index value in February–March and the low index value in April–May. Finally, model predictors also included the Normalized Difference Red Edge (NDRE; Gitelson et al., 1996) and the Normalized Difference Moisture Index (NDMI; Gao, 1996). NDRE is commonly used to measure crop health by detecting chlorophyll levels in the near-infrared and red edge parts of the electromagnetic spectrum (Equation 4). NDMI uses reflectance in the near-infrared and shortwave infrared bands to measure the water content in vegetation (Equation 5). Together, these thirteen indices provided complementary measures of

vegetation, bare soil, and moisture dynamics, enabling the random forest model to learn to distinguish winter cover crop presence and absence. Once the random forest model was trained, the team downloaded the outputs and used ArcGIS Pro 3.5 to reproject the data to the Conus Albers Equal Area Projection (EPSG 5070) to ensure accurate spatial alignment and suitability for calculations involving area.

$$\text{NDVI} = \frac{\text{NIR}-\text{Red}}{\text{NIR}+\text{Red}} \tag{1}$$

$$\text{NBR} = \frac{\text{NIR}-\text{SWIR}}{\text{NIR}+\text{SWIR}} \tag{2}$$

$$\text{BSI} = \frac{(\text{SWIR}+\text{Red})-(\text{NIR}+\text{Blue})}{(\text{SWIR}+\text{Red})+(\text{NIR}+\text{Blue})} \tag{3}$$

$$\text{NDRE} = \frac{\text{NIR-REI}}{\text{NIR}+\text{REI}} \tag{4}$$

$$\text{NDMI} = \frac{\text{NIR}-\text{SWIR1}}{\text{NIR}+\text{SWIR1}} \tag{5}$$

2.2.3 Evapotranspiration and Soil Moisture Data

Out of the four fields from the AG-CARES research site, fields 7 and 8 were both winter wheat/cotton rotations. Fields 1, 8, and 9 were chosen because of their proximity to each other. The team processed HLS data to calculate median monthly NDVI aggregated over each polygon for fields 1, 8, and 9 at the AG-CARES site from 2016 to 2024. Median monthly NDVI was aggregated for each polygon by taking the median value of the pixels in each polygon. This time period was selected to align with the availabilities of HLS data on NDVI, OpenET data, and AG-CARES management history. The OpenET evapotranspiration data were also aggregated across polygons 1, 8, and 9 by taking the monthly median OpenET value for each polygon. Landsat 8 OLI/TIRS and Landsat 9 OLI-2/TIRS-2 were merged using Google Earth Engine to provide information on land surface temperature for calculating the Soil Moisture Index (SMI). SMI uses land surface temperature to calculate the wetness of the topsoil (Equation 6). Median SMI was calculated across polygons 1, 8, and 9 individually.

$$\text{SMI} = \frac{\text{LSTmax}-\text{LST}}{\text{LSTmax}-\text{LSTmin}} \tag{6}$$

2.3 Data Analysis

2.3.1. Maryland Model

The team conducted several spatial analyses in ArcGIS Pro to assess the performance of the Maryland Model in the study area. Using the mask that separated the model outputs into a binary based on a likelihood threshold of 3, the team calculated the total percentage of cropland pixels that the Maryland Model predicted had winter cover crops. The team also conducted zonal statistics to analyze the distribution of model outputs on cropland across the eight counties, then used Microsoft Excel Version 16.103 to visualize the results as a bar chart and convert the units to acres. The team used the corn, cotton, and sorghum masks and county boundaries polygons in ArcGIS Pro to calculate the distribution of cover crop classifications per county and cash crop type. These results were then imported into RStudio Version 2025.09.0+387 to generate box plots for each county and into Excel to generate pie charts per cash crop. The team also compared the Maryland Model results with the farmer-provided field data by using ArcGIS Pro to calculate the percentage of pixels in each field polygon that the model classified as cover cropped.

2.3.2. Random Forest Model

Using the generated training data and prepared predictors, the team ran the random forest model to predict which land areas had cover crops in the winter of 2024–2025. The random forest model worked by generating many decision trees and then combining their results to make more accurate predictions. Each tree used a random subset of the training data and a random subset of the predictors to split the data at each node and ultimately make a classification on whether a pixel had a winter cover crop or not. The final prediction of whether a pixel was cover cropped or not was based on the majority vote of all the trees. The team set the model parameters to build 200 trees, with a minimum leaf population of 1 and a maximum of 50 nodes. The model used the k-fold cross-validation method for internal validation. To assess the performance of the model, the team calculated the model's distribution of cover crop classifications for the full study area as well as per 2024 cash crop and per county, following the same workflows used to analyze the Maryland model outputs. The random forest model results were also compared to the field data using the same workflow.

2.3.3. Model Comparison Analysis

To compare the outputs of the Maryland model with the team's random forest model, the team used ArcGIS Pro to identify which pixels were classified as a winter cover crop in both models. Winter cover crop presence was defined as a likelihood score of 3 or above in the Maryland model and as a positive winter cover crop detection in the random forest model. The team calculated the percentage of agreement between the models over the full study area and visualized the results as pie charts.

2.3.4. Evapotranspiration and Soil Moisture Analysis at the AG-CARES Research Site

Time series plots were generated in R version 4.4.2 for polygons 1, 8, and 9 by importing median monthly total evapotranspiration data in millimeters, median NDVI, and median SMI data. Plots were constructed comparing evapotranspiration and NDVI across the three polygons from 2016 to 2024. Correlation graphs were also constructed comparing SMI to NDVI and evapotranspiration to NDVI for all data from 2016 through 2024.

3. Results

3.1 Analysis of Results

3.1.1. Maryland Model

Overall, the Maryland Model predicted that approximately 9.5% of cropland in the study area had winter cover crops in 2024–2025 (Figure 4). Spatial analysis of the model results showed that the Maryland Model predicted there would be more winter cover crops in northern counties in the region, like Bailey, Lamb, and Hale, as compared to the southern counties like Terry, Lynn, and Dawson (Figure A1). In addition to spatial variations, the model's predicted winter cover crop likelihood scores varied depending on the cash crop planted in the preceding 2024 growing season. Areas planted with corn received much higher likelihood scores, on average, than areas planted with cotton or sorghum (Figure A2). This distribution per crop type varied spatially, as well, with corn cropland in northern counties having higher winter cover crop likelihood scores than in southern counties (Figure A3). When tested against the training data, the Maryland Model results yielded an overall accuracy of 74.9%. The model's producer's accuracy was 72%, higher than its user's accuracy of 46%. This means the model correctly identified 72% of the fields that were actually cover cropped in the training data, but only 46% of the fields the model predicted as cover cropped were truly cover cropped according to the training data. The lower user's accuracy indicated a relatively higher rate of false positives in the cover crop predictions.

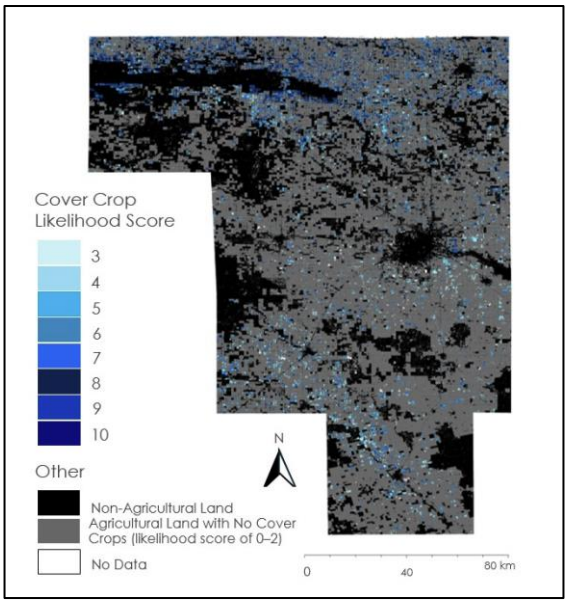

Figure 4. Results from the Maryland model for the 2024–2025 winter season, based on HLS data.

3.1.2. Random Forest Model

Over the entire study area, the random forest model predicted that 10.3% of agricultural land had winter cover crops (Figure 5). The random forest model also predicted that winter cover crops were more prevalent in northern counties, like Lamb, and Hale, than in southern counties like Terry, Lynn, and Dawson (Figure A4). The model performed relatively well when tested against the training data, with an overall accuracy of 92.6% and even performance across producer's and user's accuracy at around 91% each. The model had a Kappa coefficient of 0.84, indicating strong performance.

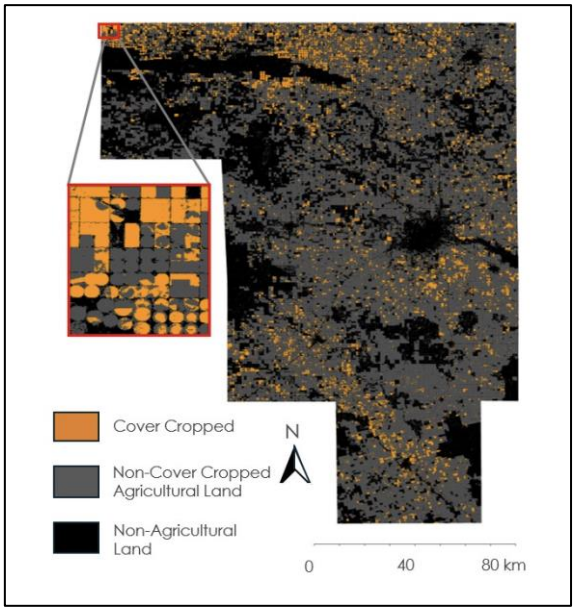

Figure 5. Results of the random forest model.

3.1.3. Model Comparison Analysis

Overall, the Maryland and random forest models agreed on classifications for the majority of agricultural land, both agreeing on winter cover crop presence for 4.3% of agricultural land and winter cover crop absence for 84.6% (Figure 6). Where they disagreed, the random forest model predicted a larger portion of

pixels had winter cover crops than the Maryland Model predicted when using a likelihood score threshold of 3 and above for the Maryland Model.

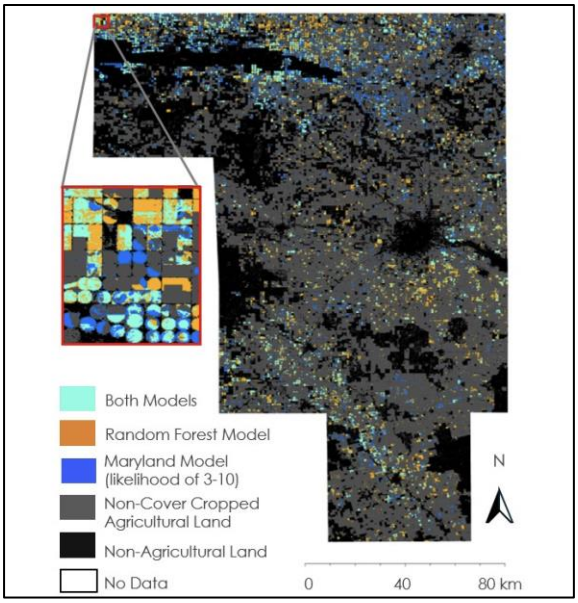

Figure 6. Results from both models overlaid, indicating areas of disagreement and agreement.

The distribution of cover crop classification per 2024 cash crop showed variation across the two models. Out of all fields planted with corn in the 2024 growing season, the Maryland model predicted that 45% had winter cover crops in the following 2024–2025 winter season, while the random forest predicted that 25% of corn fields had cover crops that winter (Figure 7). For cotton, both models predicted a similar proportion of about 6–8% of cotton fields having winter cover crops, and the models predicted about 15–22% of sorghum fields had winter cover crops.

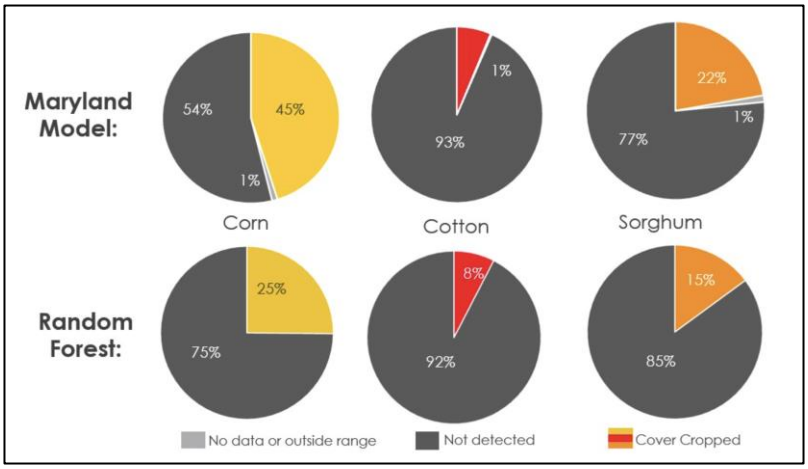

Figure 7. Pie charts representing the proportion of cropland planted with corn, cotton, and sorghum in 2024 that each model predicted had cover crops or not in the 2024–2025 winter season.

Comparing the classification predictions from both models against farmer-provided field data revealed differences in how each model classified specific fields. On the AG-CARES site, both models correctly classified fields 1 and 7 as not having winter cover crops (Figure 8). Results were more mixed for field 8, which did not have a winter cover crop, but rather winter wheat grown as a cash crop. Like a cover crop, winter wheat covered the field in the winter, but unlike a cover crop, winter wheat was not terminated in the

spring but instead continued to grow until summer harvest. The random forest model incorrectly classified field 8 as cover cropped, suggesting that the model was unable to detect that the field had not been terminated in the spring. The Maryland Model's performance for field 8 depended on the threshold set for the likelihood score. If the threshold was 3, the model correctly classified as the field as not being winter cover cropped, but if lowered to 1 or 2, the model would have incorrectly classified it as winter cover cropped. For field 9, the random forest model correctly classified the field as being winter cover cropped, whereas the Maryland Model's classification again depended on the likelihood threshold. For the five operational fields where farmers provided management data for 2024–2025, the Maryland Model with a likelihood threshold of 3 correctly classified one field, whereas the random forest model correctly classified three out of the five based on the predominant classification of pixels within the field boundaries (Table 4). Lowering the Maryland Model threshold would not have changed the overall field-level classifications for these fields, based on the majority pixel class per field boundary.

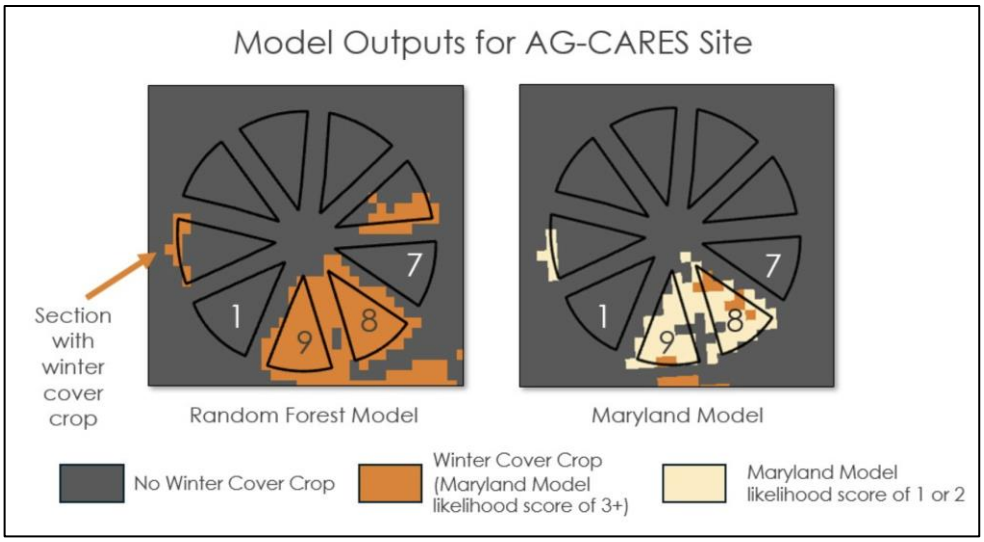

Figure 8. Model results for the AG-CARES site. Fields 1 and 7 did not have a winter cover crop, field 9 did have a winter cover crop, and field 8 had winter wheat that was not a cover crop but grown for harvest.

Table 4.
Model Results for Fields with Management Data

Winter Cover Crop per Management Data (Yes/No)	Maryland Model (% pixels predicted as cover cropped)	Random Forest Model (% pixels predicted as cover cropped)
No	**No (0%)**	**No (0%)**
Yes	No (7%)	No (43%)
Yes	No (0%)	No (4%)
Yes	No (12%)	**Yes (100%)**
Yes	No (2%)	**Yes (100%)**

3.1.4. Evapotranspiration and Soil Moisture Case Study Analysis at the AG-CARES Research Site
The case study analysis of the AG-CARES site showed that evapotranspiration generally followed NDVI trends. Field 9 had a double peak in NDVI for both the cash crop peak and the cover crop peak (Figure 9). The median total annual evapotranspiration values over the nine-year study period indicated that in this case study, the cover cropped field, field 9, experienced the highest evapotranspiration (Table A3). Case study results showed that higher NDVI was correlated with higher evapotranspiration. For soil moisture, there was no correlation between soil moisture and NDVI (Figure 10).

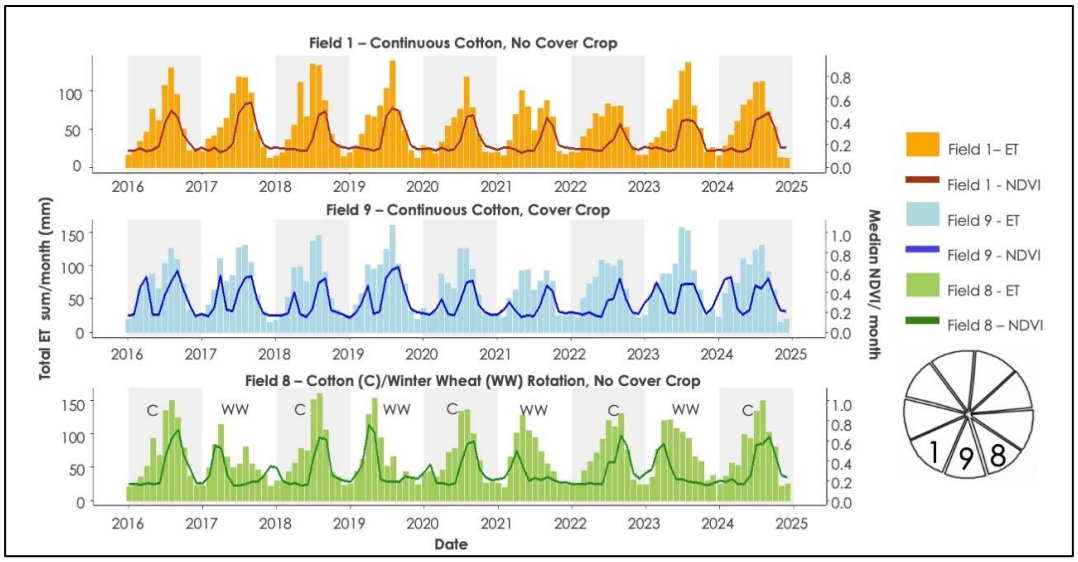

Figure 9. Three time series graphs showing the relationships between NDVI and ET from 2016–2024 on fields 1, 9, and 8.

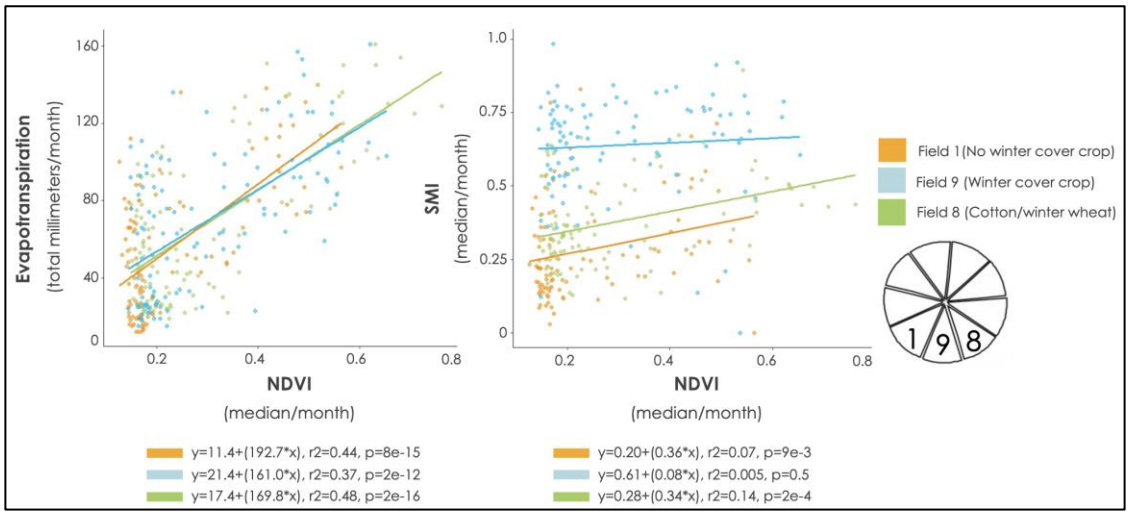

Figure 10. A time series graph showing the correlation between NDVI and evapotranspiration, as well as NDVI and soil moisture.

3.2 Errors & Uncertainties

At the time this study was conducted, the Maryland Model was still under development and unpublished, so the team had a relatively limited understanding of its parameters. This uncertainty complicated interpretation of its results. The random forest model was also limited by being trained on data derived from visual interpretation of true-color satellite imagery rather than field data. As a result, the training data may have included misclassified pixels. Cover crops that were not visibly green in the imagery might have been missed, while weeds or residue that appeared green might have been wrongly labeled as cover crops.

For the model comparison, direct evaluation of performance metrics between the two models was limited by the inherent bias in how the performance metrics were calculated. Accuracy measurements were derived by comparing each model's outputs to the training data that was used to train the random forest model. The team-generated training data was not used in training the Maryland Model. Consequently, it was expected that the random forest model exhibited higher accuracy due to inherent bias in the comparison method.

Both models classified land at the pixel level, which restricted direct translation to field-scale assessments across the study area. Both models indicated that areas planted with corn were more likely to have winter cover crops, but the project partners noted these results did not align with their knowledge of growing practices in the study area. The models may have incorrectly detected other vegetation signals such as weeds or residue; further exploration would be necessary to better understand model behavior on corn cropland. More field data would be needed to improve the training, performance, validation, and interpretation of both models. For the evapotranspiration and soil moisture assessments, analysis was limited to a single research site as a case study, so results from this case study cannot be generalized to the broader region.

4. Conclusions

4.1 Interpretation of Results

Both the random forest model and Maryland Model showed that winter cover crops in the Southern High Plains of Texas are detectable via remote sensing, but further refinement would be needed before adopting these workflows to accurately map cover cropping practices in the region. As the results from the Maryland Model on the AG-CARES site showed, using the same winter cover crop likelihood threshold as in Maryland reduced accuracy under west Texas conditions. The random forest model results showed that incorporating a diversity of vegetation and soil indices, such as BSI and NBR, improved cover crop detection accuracy. In a semi-arid region like west Texas, vegetation indices typically exhibit lower values, so cover crop models that depend on these indices must be adjusted accordingly for accurate detection. Accurate identification of cover crop termination was also critical for reliable mapping. As the results from the model comparison on the AG-CARES site showed, fields with winter crops that were not terminated but rather grown for harvest posed challenges for classification. Refining termination detection would improve model accuracy. Field data on cover crop performance, planting dates, and termination dates proved essential for adapting model parameters to seasonal vegetation patterns in the region. Field observations from farmers indicated that visually inspecting vegetation in February and May aligned with the timing of cover crop vegetation peaks and termination. Field data also indicated that successful cover crops in the area sometimes did not appear visibly green, which informed the visual classification process. Training cover crop classification models on a large quantity of field data, rather than visual interpretations of imagery, would improve true winter cover crop detection. Finally, preliminary results from satellite-derived evapotranspiration and soil moisture data showed that cover crops impact water availability, but further validation would be needed.

4.2 Feasibility & Partner Implementation

This feasibility study generated results that our partners can apply and integrate into their ongoing work. Broadly, this feasibility study advances the collaboration between NASA and the partners to support agricultural communities in the Southern High Plains of Texas, providing a foundation for further development of cover crop mapping in the region. SARA, Bamert Seed Company, and Texas A&M AgriLife will benefit from the exploration of use cases for NASA Earth observations for agricultural decision-making in the region, which can inform future research, initiatives and partnerships. Collaborators at the USDA-ARS and USGS can use the results from the model analyses to refine the Maryland Model parameters to better match Texas conditions. These findings, along with the gathered field data and insights on regional practices, trends, and planting dates, will guide the adaptation and validation of the Maryland Model for the Southern High Plains of Texas. Texas A&M AgriLife will also benefit from the results of the AG-CARES case study, which provides nine years of monthly, seasonal, and annual evapotranspiration and soil moisture data. These outputs will enable comparisons between satellite-derived and in-situ measurements at AG-CARES, supporting Texas A&M AgriLife's research into water resource management and crop sustainability. Overall, this project allows partners to further explore remote sensing techniques to understand winter cover crop dynamics in the region to inform sustainable crop management decisions.

5. Acknowledgements

The Southern High Plains Texas Agriculture team would like to thank our partners, Tillery Timmons-Sims (SARA), Rob Cook (Bamert Seed Company), and Katie Lewis (Texas A&M AgriLife Research), for their thoughtful collaboration, input, and essential coordination for gathering field data. We are deeply grateful to every farmer who contributed data. We thank Dr. Feng Gao, Dr. Dean Hively, and Dr. Jyoti Jennewein for allowing us to experiment with applying their developing model to a new region. We are grateful to our Leads, Kaitlyn Lemon and Truman Anarella, as well as our Science Advisors at Colorado State University, Dr. Anthony Vorster, Dr. Paul Evangelista, and Christopher Tsz Hin Choi, for their invaluable support and guidance throughout the term. We also thank Alison Thieme at the University of Maryland for sharing her expertise and Dr. Christopher Cobos of AgriLife for generously sharing his dissertation data on AG-CARES management history.

This material contains modified Copernicus Sentinel data (2016–2025), processed by ESA.

Any opinions, findings, and conclusions or recommendations expressed in this material are those of the author(s) and do not necessarily reflect the views of the National Aeronautics and Space Administration.

This material is based upon work supported by NASA through contract 80LARC23FA024.

6. Glossary

AG-CARES – Agricultural Complex for Advanced Research and Extension Systems
ARS – Agricultural Research Service
BSI – Bare Soil Index
CDL – Cropland Data Layer
Cover crop – a crop grown specifically for ecological benefits rather than for harvest
dNBR – differenced Normalized Burn Ratio
Earth observations – Satellites and sensors that collect information about the Earth's physical, chemical, and biological systems over space and time
ESA – European Space Agency
Evapotranspiration (ET) – the combined processes that move water from the Earth's surface into the atmosphere, including evaporation from surfaces like soil as well as transpiration from plants
HLS – Harmonized and Landsat Sentinel-2
Kappa coefficient – A statistic used to measure the agreement between two classifiers
Maryland Model – Winter cover crop detection algorithm under development by researchers at the USDA-ARS and USGS
MSI – Multispectral Instrument
NDMI – Normalized Difference Moisture Index
NDRE – Normalized Difference Red Edge

NDVI – Normalized Difference Vegetation Index
OLI – Operational Land Imager
Producer's accuracy – Measure of how often real-world features are correctly identified by a classifer
Random forest – Ensemble machine learning model that builds multiple decision trees and determines a final classification by aggregating predictions from all trees
SARA – Sandhills Area Research Association
SMI – Soil Moisture Index
TIRS – Thermal Infrared Sensor
USDA – United States Department of Agriculture
User's accuracy – Measure of how often a pixel classified as a particular class by a classifier actually corresponds to that class on the ground
USGS – United States Geological Survey

7. References

Ahmed, Z., Nalley, L., Brye, K., Green, V. S., Popp, M., Shew, A. M., & Connor, L. (2023). Winter-time cover crop identification: A remote sensing-based methodological framework for new and rapid data generation. *International Journal of Applied Earth Observation and Geoinformation*, *125*, Article 103564.

Allen, R. G., Tasumi, M., & Trezza, R. (2007). Satellite-based energy balance for mapping evapotranspiration with internalized calibration (METRIC)—Model. *Journal of Irrigation and Drainage Engineering, 133*(4), 380-394. https://doi.org/10.1061/(ASCE)0733-9437(2007)133:4(380)

Allen, V. (2004). Sustainable Crop/Livestock Systems in the Texas High Plains: Final Report for LS97-082 - SARE Grant Management System. Sare.org. https://projects.sare.org/project-reports/ls97-082/

Baxter, L. L., West, C. P., Brown, C. P., & Green, P. E. (2021). Cover crop management on the Southern High Plains: Impacts on crop productivity and soil water depletion. *Animals 11*(1), 212. https://doi.org/10.3390/ani11010212

Cronin, J. G., & Myers, B. N. (1964). A summary of the occurrence and development of ground water in the Southern High Plains of Texas (No. 1693). US Geological Survey. https://doi.org/10.3133/wsp1693

Gao, B.C. (1996). NDWI—A normalized difference water index for remote sensing of vegetation liquid water from space. *Remote Sensing of Environment 58*(3), 257–266. https://doi.org/10.1016/S0034-4257(96)00067-3

Gitelson, A. A., Kaufman, Y. J., & Merzlyak, M. N. (1996). Use of a green channel in remote sensing of global vegetation from EOS-MODIS. *Remote Sensing of Environment, 58*(3), 289–298. https://doi.org/10.1016/S0034-4257(96)00072-7

Hampel, F.R. (1974). The influence curve and its role in robust estimation. *Journal of the American Statistical Association*, 69(346), 383–393. https://doi.org/10.1080/01621459.1974.10482962

Hively, W. D., Duiker, S., McCarty, G., & Prabhakara, K. (2015). Remote sensing to monitor cover crop adoption in southeastern Pennsylvania. *Journal of Soil and Water Conservation, 70*(6), 340 352. https://doi.org/10.2489/jswc.70.6.340

Key, C.H. & Benson, N.C. (2006). Landscape Assessment: Ground Measure of Severity, the Composite Burn Index; and Remote Sensing of Severity, the Normalized Burn Ratio. In FIREMON: Fire Effects Monitoring and Inventory System.

Laipelt, L., Kayser, R. H. B., Fleischmann, A. S., Ruhoff, A., Bastiaanssen, W., Erickson, T. A., & Melton, F. (2021). Long-term monitoring of evapotranspiration using the SEBAL algorithm and Google Earth Engine cloud computing. *ISPRS Journal of Photogrammetry and Remote Sensing*, *178*, 81-96. https://doi.org/10.1016/j.isprsjprs.2021.05.018

Masek, J., Ju, J., Roger, J., Skakun, S., Vermote, E., Claverie, M., Dungan, J., Yin, Z., Freitag, B., & Justice, C. (2021). HLS Operational Land Imager Surface Reflectance and TOA Brightness Daily Global 30m (Version 2) [Data set]. NASA EOSDIS Land Processes DAAC. Retrieved October 23, 2025, from https://doi.org/10.5067/HLS/HLSL30.002

Melton, F., Huntington, J., Grimm, R., Herring, J., Hall, M., Rollison, D., Erickson, T., Allen, R., Anderson, M., Fisher, J., Kilic, A., Senay, G., Volk, J., Hain, C., Johnson, L., Ruhoff, A., Blankenau, P., Bromley, M., Carrara, W., Daudert, B., Doherty, C., Dunkerly, C., Friedrichs, M., Guzman, A., Halverson, G., Hansen, J., Harding, J., Kang, Y., Ketchum, D., Minor, B., Morton, C., Revelle, P., Ortega-Salazar, S.,

Ott, T., Ozdogon, M., Schull, M., Wang, T., Yang, Y., & Anderson, R. (2021.) [Data set]. OpenET: Filling a Critical Data Gap in Water Management for the Western United States. *Journal of the American Water Resources Association 58*(6): 971–994. https://doi.org/10.1111/1752-1688.12956

Rikimaru, A., Roy, P. S., & Miyatake, S. (2002). Tropical forest cover density mapping. *Tropical Ecology 43*(1), 39–47.

Rouse, J. W., Haas, R. H., Schell, J. A., & Deering, D. W. (1973). Monitoring Vegetation Systems in the Great Plains with ERTS. NASA SP-351, 309–317.

Soil Health Institute. (2023, June). *USRCF fact sheet: Texas High Plains* [PDF]. Soil Health Institute. https://soilhealthinstitute.org/app/uploads/2023/06/USRCF-Fact-Sheet_Texas-High-Plains.pdf

Texas Almanac. (2021). *Soils of Texas*. Texas Almanac. https://www.texasalmanac.com/articles/soils-of-texas

Texas Department of Transportation. (2025). Texas County Boundaries Detailed. [Data set]. https://gis-txdot.opendata.arcgis.com/datasets/texas-county-boundaries-detailed/explore.

Texas Parks and Wildlife Department. (n.d.). *High plains*. Texas Parks & Wildlife Department. https://tpwd.texas.gov/wildlife/wildlife-diversity/wildscapes/wildscapes-plant-guidance-by-ecoregion/high-plains/

USDA National Agricultural Statistics Service. (2024). Cropland Data Layer. [Data set]. USDA-NASS. Retrieved October 23, 2025, from https://nassgeodata.gmu.edu/CropScape/

Yousefi, M., Dray, A., & Ghazoul, J. (2024). Assessing the effectiveness of cover crops on ecosystem services: a review of the benefits, challenges, and trade-offs. *International Journal of Agricultural Sustainability, 1*, Article 2335106. https://doi.org/10.1080/14735903.2024.2335106

Appendix A: Additional Tables and Figures

Table A1

OpenET evapotranspiration models used to calculate the Ensemble value

OpenET Ensemble Models
LEXI/DisALEXI (version 0.0.32)
eeMETRIC (version 0.20.26)
geeSEBAL (version 0.2.2)
PT-JPL (version 0.2.1)
SIMS (version 0.1.0)
SSEBop (version 0.2.6)

Table A2

Predictors for the random forest model

Median NDVI	Median NDVI difference between February and May
NDVI maximum in previous summer	NDVI minimum in previous summer
NDVI maximum in winter (before February)	Difference between NDVI high in Feb-March and NDVI low April-May
NDVI minimum in winter (before February)	dNBR between February and May
NDMI	NDRE
BSI difference between February and May	Difference between BSI high in Feb-March and BSI low April-May
Difference between NBR high in Feb-March and NVR low April-May	

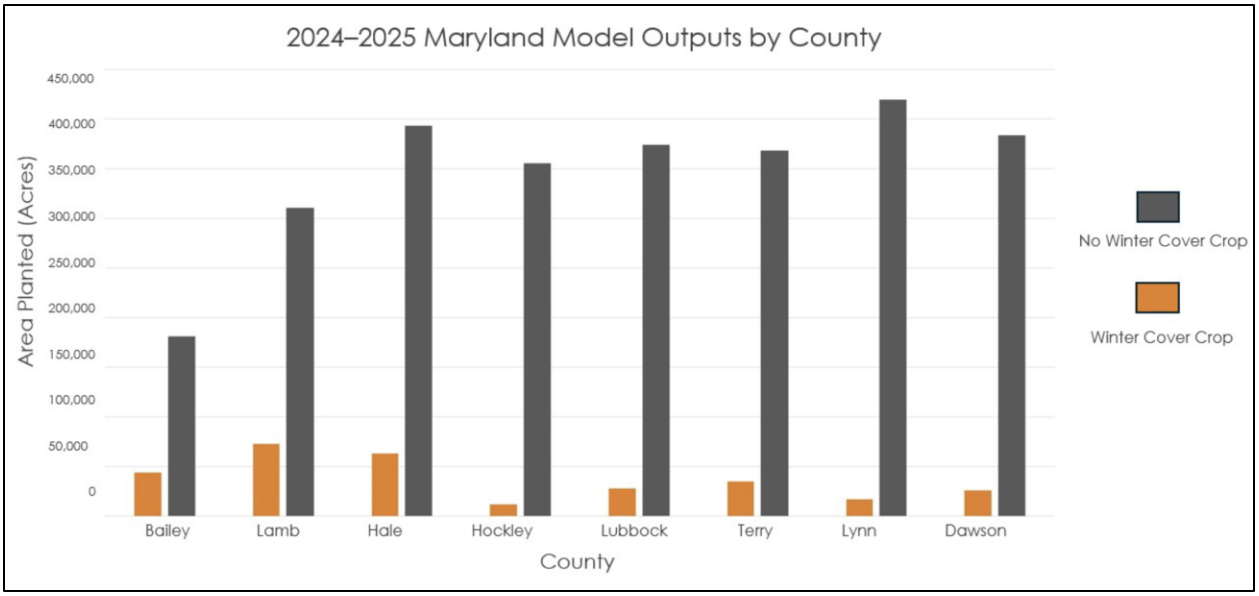

Figure A1. Bar chart of the distribution of areas the Maryland Model predicted for winter cover crop presence and absence, by county.

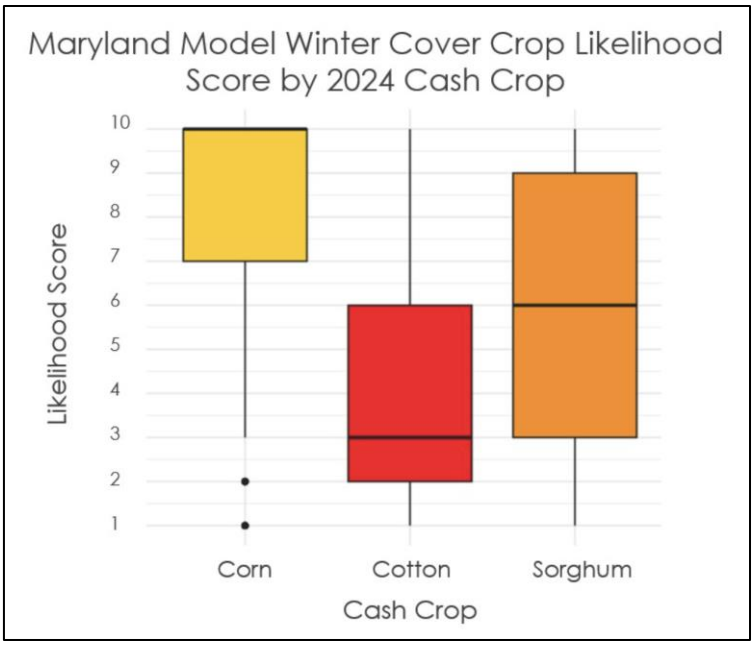

Figure A2. Box plot indicating the distribution of 2024–2025 winter cover crop likelihood scores that the Maryland model applied to pixels planted with corn, cotton, and sorghum in the 2024 growing season.

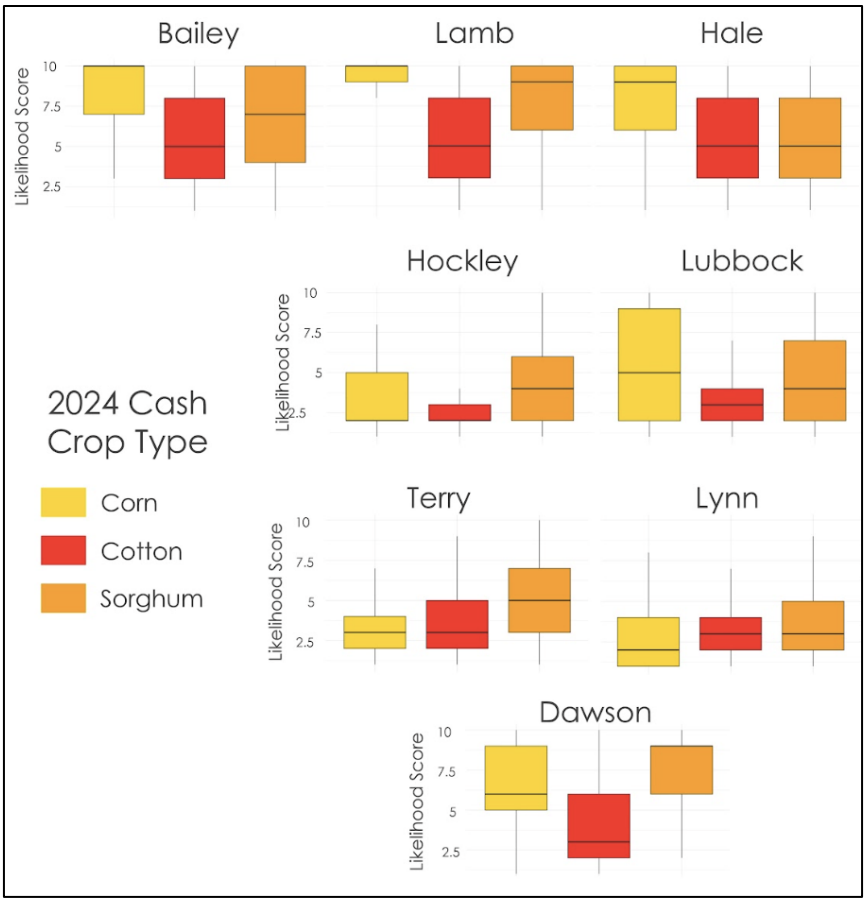

Figure A3. Distribution of 2024–2025 winter cover crop likelihood scores from 1 to 10 that the Maryland model assigned for pixels that were planted with corn, cotton, or sorghum in 2024.

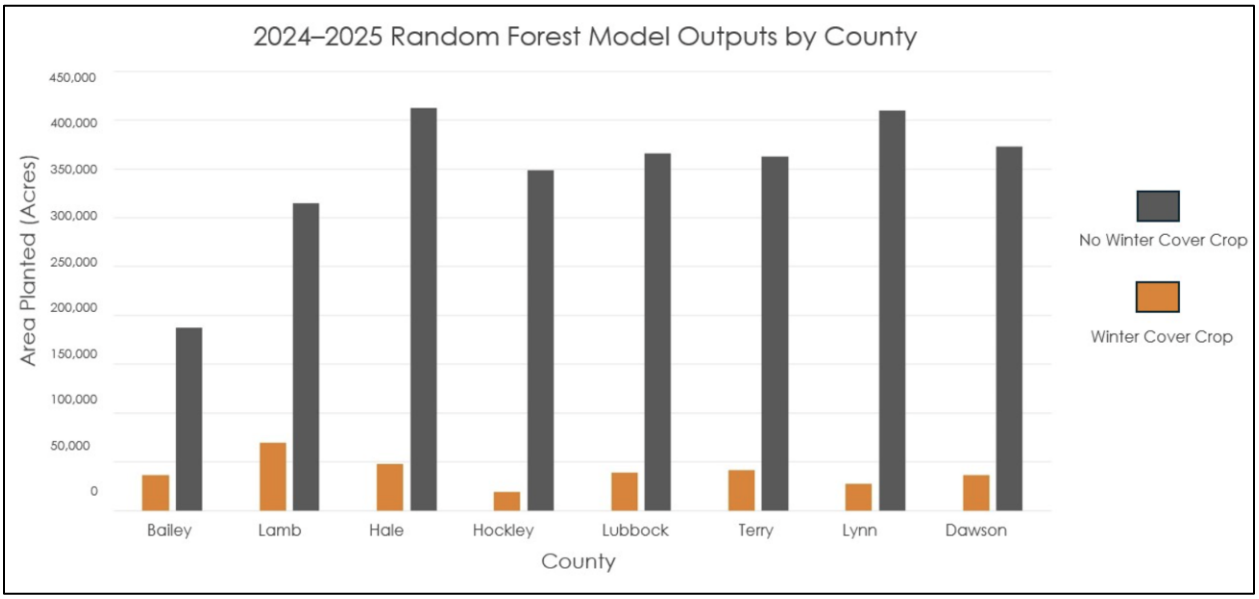

Figure A4. Bar chart of the distribution of areas the random forest model predicted for winter cover crop presence and absence, by county.

Table A3

Yearly ET totals (mm). Winter wheat years are highlighted for field 8 as those are the years with winter cover.

Year	**No Cover Crop - Continuous Cotton (1)**	**Cover Crop – Continuous Cotton (9)**	**No Cover Crop - Winter Wheat/Cotton Rotation (8)**
2016	679 mm	821 mm	829 mm
2017	712 mm	859 mm	690 mm
2018	743 mm	836 mm	832 mm
2019	701 mm	925 mm	745 mm
2020	570 mm	783 mm	796 mm
2021	640 mm	697 mm	766 mm
2022	599 mm	791 mm	804 mm
2023	739 mm	958 mm	872 mm
2024	692 mm	892 mm	892 mm
Median	692 mm	836 mm	804 mm